Journal of Petroleum Science and Technology 15(1): 45, 2025, Pages 2-14
DOI:10.22078/jpst.2026.5665.1973

Journal of Petroleum Science and Technology

Research Paper

https://jpst.ripi.ir/

Absolute Permeability Upscaling Assessment in Different Coarsening Levels in Reservoirs with Various Heterogeneities and Displacement Processes

Ali Asghar Movahed[1], Mohammad Reza Rasaei*[2] and Khalil Shahbazi[3]

1. Ahvaz Research Center, Faculty of Research &. amp; Development of Upstream Petroleum Industry, Research Institute of Petroleum Industry, Tehran, Iran

2. Institute of Petroleum Engineering, School of Chemical Engineering, College of Engineering, University of Tehran, Tehran, Iran

3. Ahvaz Faculty of Petroleum, Petroleum University of Technology, Ahvaz, Iran

Abstract
Upscaling is an effective solution to overcome time and resource limitations in dynamic reservoir simulation. In this study, eight absolute permeability upscaling methods were evaluated, namely: arithmetic, geometric, harmonic-arithmetic, renormalization, pressure-solver, unbiased, sequential unbiased, and sequential pressure-solver methods. The last three methods, introduced here for the first time, are numerical approaches in which the diffusivity equation is solved over local fine grid-blocks under the corresponding boundary condition of the coarse grid-blocks, and the equivalent permeability is then calculated using Darcy's equation. By implementing six water-flooding scenarios over three synthetically generated reservoirs, the effects of a broad range of mobility ratios (0.2 to 20), capillary pressure, and reservoir heterogeneity on the performance of upscaling methods were investigated. Moreover, it was observed that average boundary pressure errors were high and increased rapidly with up-scaling level from 2% at level 2 to 35% at level 16. Furthermore, a similar trend was observed for the average reservoir pressure, but it has much smaller error which goes up to 7% at highest upscaling level. Therefore, it is necessary to apply near-well/boundary upscaling methods to improve pressure distribution. The overall error never exceeded 0.5% with respect to heterogeneity and capillary pressure effects, whereas at MR = 0.2, it increased to about 5–6% for oil and 1.5% for water production rate. In most scenarios, numerical methods produced smaller overall error compared with analytical methods. Ultimately, in general, unbiased and sequential unbiased estimation were found to be the superior numerical methods and arithmetic and harmonic-arithmetic methods were identified as the superior analytical methods.

Keywords: Upsscaling, Absolutes Permeability, Analytical Method, Numerical Method, Heterogeneity, Displacement Process.

Introduction
Flow simulations of multimillion-block geological models are almost impossible due to computer hardware limitations and calculation time. Up-scaling proved to be the most effective solution to overcome these limitations. In general, porosity, fluid saturation, absolute and relative permeability, capillary pressure and/or any petrophysical parameter can be up-scaled. Although certain methods exist for up-scaling additive parameters such as porosity and fluid saturation, the same is not true for other important non-additive parameters such as absolute permeability and multi-phase saturation functions.
Many methods are proposed for absolute permeability up-scaling since 1960. Simple arithmetic, harmonic, and geometric averaging methods were applied by many researchers such as Matheron [1], Muskat [2], Bouwer [3], Warren and Price [4], Dagan [5-7], and Clifton and Neuman [8]. These methods are specific cases of a more general approach of power averaging presented by Journel et al. [9]. Moreover, combinations of these simple methods named as arithmetic-harmonic and harmonic-arithmetic were examined by Durlofsky [10], Lozano et al. [11], and Pickup and Sorbie [12]. By using a simple two-layer model, Sharifi and Kelkar [13] developed an analytical expression for the effective permeability as a function of time. They showed that for later times of production, the effective permeability is not only a function of permeability, but also porosity of the fine scale model. Hsieh et al. [14] utilized layered equivalent permeability technique, through which horizontal and vertical upscaled permeabilities of the composite hydrofacies (CHFs) were determined by arithmetic and

**Corresponding author:* Mohammad Reza Rasaei, *Institute of Petroleum Engineering, School of Chemical Engineering, College of Engineering, University of Tehran, Tehran, Iran*
E-mail addresses: mrasaei@ut.ac.ir
Received 2025-04-10, Received in revised form 2026-05-09, Accepted 2026-08-25, Available online .....

harmonic averaging of the included hyrofacies (HFs) corresponding permeabilities, respectively. Using analogy of fluid flow and electrical conductance, King [15] proposed a different averaging technique known as renormalization. Green and Paterson [16] suggested a simple analytical approximation to the method of renormalization in three dimensions. On the basis of the structure of the exact two-dimensional renormalization method, an analogous three-dimensional scheme was proposed by Karim and Krabbenhoft [17]. Liao et al. [18, 19] proposed an analytical method in which perturbation expansion and Fourier Analysis are utilized. Above mentioned analytical methods have the advantage of simple implementation and fast computation, but they are limited to simple and low-degree heterogeneity patterns. Numerical methods are proposed to overcome this limitation by solving diffusion equation over fine grid blocks. Gomez-Hernandez [20], Sanchez-Vila [21], Warren and Price [4], White and Horne [22], Pickup and Sorbie [12], Lunati et al. [23], and Durlofsky [10] proposed different numerical approaches. Details of these methods can be found in rich review papers published by MacCarthy [24], Wen and Gomez-Hernandez [25], Renard and Marsily [26], and Durlofsky [27].

Chen et al. [28] and Chen and Durlofsky [29] proposed local-global upscaling approach for simulating heterogeneous formations. A non-local three-dimensional hydraulic conductivity full tensor upscaling algorithm was suggested by Zhou et al [30]. Authors proposed computing directly the interblock conductivity during the upscaling process thus avoiding the need to average already averaged (upscaled) values of adjacent blocks. Chen [31] developed a new upscaling procedure generating coarse-scale transmissibilities directly. Dagan et al. [32] clarified a few issues of principle and discussed open questions about upscaling. Some studies were implemented for estimating effective or equivalent conductivity (Suribhatla et al. [33]; Jankovic et al. [34]). Fouda [35] discussed the findings of single-phase upscaling emphasizing that the results of numerical methods are affected by boundary conditions of coarse blocks. Evazi and Jessen [36] proposed a dual-porosity upscaling approach in which the pore space is arranged into two levels of porosity based on flow contribution, and a dual-porosity dual-permeability flow model is adapted for coarse-scale flow simulation. Based on the flux conservation, Failla, [37] suggested a numerical upscaling technique which looks for the upscaled permeability values that kept the flux constant across the coarse block boundary. Thereafter, Mazo and Potashev [38] suggested a method through which, full upscaled permeability tensor was determined by minimizing the mismatch between fine-scale and coarse-scale face fluxes. Li and Durlofsky [39] implemented transmissibility upscaling in addition to considering near-well effects and upscaling other dynamic parameters. Moreover, some authors either debated about or presented new techniques for transmissibility upscaling (Vitel and Souche [40]; Lambers et al. [41]; Chen [31]; Azmi et al. [42]; Guérillot and Bruyelle [43,44]; Alpak [45]). Stone et al. [46] suggested new techniques to calculate flow in isolated bodies and how to imbed these solutions into a global upscaling framework was discussed.

To address the upscaling of thermal–compositional simulations regarded to SAGD oil recovery process, Kumar [47] and Kumar et al. [48] developed a statistical upscaling approach that utilized geometrical averaging to derive the upscaled horizontal permeability. A physics-based scheme was proposed by Murugesu [49] in which the upscaled permeability was determined such that minimized the pressure difference between the fine scale and coarse scale solutions corresponding to a novel proposed global boundary conditions encountered during the SAGD process. Furthermore, Tan et al. [50] suggested an upscaling method which employed scale factors, defined as the ratio of the coarse-scale grid sizes to the fine-scale grid sizes, to adjust the oil viscosity–temperature relationships in coarse-scale models.

It is noteworthy that upscaling techniques, commonly using renormalization, have been employed in some investigations to determine the equivalent permeability of digital porous media by scaling from micro-scale up to macro-scale (Dehghan Khalili [51]; Bashtani et al. [52]; Elmorsy et al. [53]).

Many up-scaling methods have already been developed, but fewer comparison studies have been done. The aim of this study is to evaluate different up-scaling methods under various heterogeneity and flow conditions to introduce superior methods in terms of minimum average error. Eight upscaling method including arithmetic, geometric, harmonic-arithmetic, renormalization, pressure-solver, unbiased, sequential pressure-solver, and sequential unbiased would be investigated. Also, six water flooding scenarios would be performed over three synthetically generated reservoirs including grid-blocks to evaluate upscaling methods under various conditions of heterogeneity, broad range of mobility ratios from 0.2 to 20 with and without capillary pressure. A two-phase and two-dimension simulator has been developed to implement flooding scenarios. Up-scaling relative permeability is not elaborated in the work because it becomes important at a very high coarsening level, i.e. from core scale to geological model scale (Durlofsky [54]).

Materials and Methods

Four analytical and four numerical up-scaling methods are considered in this paper. Only uniform coarsening of the fine models is performed. This is to put the methods under stringent tests without improvements due to advanced gridding. These methods are explained below.

Analytical Upscaling Methods

In these methods, absolute permeability of coarse block is calculated using closed analytical formula:

Arithmetic (A)

Coarse block permeability is arithmetic average of its background fine blocks permeabilities. This method returns the upper limit for up-scaled permeabilities.

Geometric (G)

Geometric average of a coarse block covering n fine blocks is the nth root of their multiplication.

Harmonic-Arithmetic (HA)

In this method, harmonic average of permeability of serial fine blocks in each row is first calculated and devoted to middle-coarse blocks. This results in some parallel longitudinal coarse blocks. Furthermore, the permeability of final coarse block is obtained by arithmetically averaging these parallel middle-coarse blocks.

Renormalization (R)

King [13] used this method for the first time to obtain coarse block permeability. The method is patterned from a 2×2 lattice of electrical resistances. In addition, ist gives a formula for equivalent permeability of a 2×2 lattice. Moreover, it can be used iteratively to calculate excessively coarser block permeabilities. For example, a D-dimensional lattice, including 2×2 blocks, is changed to a coarse one with $2^{(m-1)D}$ blocks after one stage of up-scaling where m is the number of up-scaling levels. A single coarse block will be obtained after m levels of up-scaling.

In case the areas of the fine blocks are different, then they should be considered as weight factors in analytical methods mentioned above.

Numerical Upscaling Methods

Regarding to selected region of upscaling, numerical methods generally refer to as local, extended local, global, and local-global (quasi global), which have been discussed in the literature (e.g. Durlofsky [54]; Chen et al. [28]; Chen and Durlofsky [29]; Fouda [35]). Local methods, in which a region of fine blocks is selected and parameters of coarse block are determined, were addressed in this study (See Fig. 1). In these methods, it is required to solve single-phase steady-state diffusivity equation (Equation 1) over fine blocks:

$$\nabla.(\frac{1}{\mu}/\text{k}\ \nabla\text{P})=\text{Q} \tag{1}$$

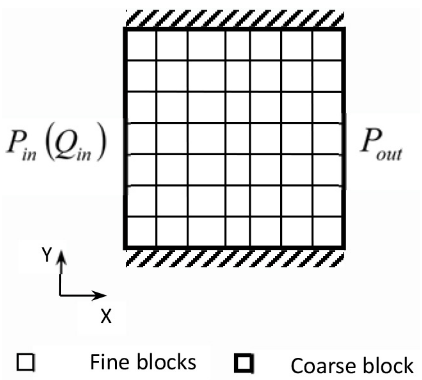

Fig. 1 Flow and no-flow boundaries related to numerical methods for calculation of coarse block permeability in *x* direction.

where μ is viscosity, k is permeability tensor, P is pressure, and Q is source/sink flow rate. The boundary and initial conditions are needed to solve diffusivity equation. Fig. 1 shows flow and no-flow boundaries of a lattice of fine blocks which its equivalent permeability is calculated in x direction. The rotation of boundary conditions results in coarse block permeability in direction. Various boundary conditions have been proposed for different numerical approaches, some of which are described below:

Pressure-solver (PS)

Constant pressures are set at the input (Pin) and output (Pout) boundaries. Pressure distribution and flow rate through fine blocks are then calculated. Furthermore, coarse block permeability is obtained by direct application of Darcy's law on total pressure gradient (P_{in}-P_{out}) and sum of fine blocks flows (Q) at inlet or outlet boundary (Inlet and outlet flow rate are equal for steady state flow); in addition, Equations 2-a, 2-b and 3 are presented below:

$$q_j = \frac{2k_j A_j}{\mu}\frac{(P_i n - P_j)}{\Delta x_j} \quad (2-a),\quad Q=\sum_{j=1}^{n} q_j$$

$$(2-b)\ K = \frac{Q\times\mu\times\Delta X}{A\times(P_{in}-P_{out})} \tag{3}$$

where q_j is flow rate, Δx_j is length, k_j is permeability, P_j is pressure, A_j is cross sectional area of fine block j at inlet boundary, ΔX is length, K is upscaled permeability, and A is cross sectional area of coarse block.

Unbiased (U)

Unbiased (U) method is almost the same as PS method, except that the inlet boundary is constant flow (Q_{in}) instead of constant pressure. This is to modify unrealistic uniform pressure gradient that appears in PS method and can produce unrealistic high flow rate in some layered permeability heterogeneities. We borrow the idea from two-phase up-scaling method proposed by Wallstorm et al. [55] and apply it to upscale absolute permeability for the first time.

Considering boundary conditions (Q_{in} and P_{out}) and calculating input flow rate q_j for each fine block, diffusivity equation can be solved over fine blocks. In addition, obtained pressure distribution of fine scale lattice, inlet boundary pressure (P_{in}) and upscaled permeability K can be calculated by averaging inlet pressure (p_j) of boundary fine blocks and using Darcy's law as follows:

$$p_j = P_j + \frac{q_j u}{A_j k_j}\frac{\Delta x_j}{2} \quad (5-a),\quad P_i n = \frac{1}{n}\sum_{j=1p_j}^{n}$$

$$(5-b)K = \frac{Q_{in}\times\mu\times\Delta X}{A\times(P_{in}-P_{out})} \tag{4}$$

In Equation 4, Δ_{yj} is width of fine block j at inlet boundary and ΔY is width of coarse block.

Sequential Pressure-Solver (SPS), and Sequential Unbiased (SU)

Sequential pressure-solver (SPS), and sequential unbiased (SU) methods can be thought of as a combination of either PS or U boundary conditions with renormalization method, respectively. Instead of calculating coarse block permeability in single step, we do it sequentially in the same way—we did in renormalization method. There are some coarse blocks obtained in each stage between fine blocks and final coarse block. Moreover, fine blocks are first up-scaled to a lattice of middle-coarse blocks. Then, obtained lattice is up-scaled to the next step coarser blocks. The procedure is continued until final coarse block obtained. Also, pressure solver and unbiased boundary conditions are applied in each coarsening stage in SPS and SU methods, respectively. In this study, unbiased, sequential unbiased and sequential pressure-solver methods are investigated for the first time in the case of absolute permeability upscaling, although similar methods might be used in the case of two-phase upscaling before. In this study, in fact, it is supposed to examine the impact of these methods on absolute permeability upscaling.

Numerical Simulator

Fine and coarse models are input data of a simulator to obtain production performance curves as well as pressure and saturation distribution for all scenarios. Then, performance curves of coarse and fine models would be compared for all scenarios to evaluate the efficiency of up-scaling methods. In this study, we developed a two-dimension, two-phase simulator in which, implicit pressure, explicit saturation (IMPES) formulation was applied to solve pressure and saturation equations. No well is considered and injection and production are performed at flow boundaries. Relative permeability of wet and non-wet phases is obtained from Corey relation (Equations 7-a and 7-b):

$$k_{rnw} = k_{rnw0}\left(\frac{1-S_w-S_{nwr}}{1-S_{wr}-S_{nwr}}\right)^{n_{nw}} \quad (7\text{-a})$$

$$k_{rw} = k_{rw0}\left(\frac{S_w-S_{wr}}{1-S_{wr}-S_{nwr}}\right)^{n_w} \quad (7\text{-b})$$

where, K_{rnw} and K_{rw0} are maximum relative permeability of non-wet and wet phases; is saturation exponent and and are residual saturations. Advanced TVD numerical dispersion control method was applied in relative permeability calculation at blocks interfaces [56]. Capillary pressure is obtained by Brooks-Corey correlation (Equation 8):

$$P_c = P_{th}\left(\frac{S_w-S_{wr}}{1-S_{wr}}\right)^{\left(-\frac{1}{\lambda}\right)} \quad (8)$$

P_{th} is threshold pressure and λ is positive number which depends on pore size distribution. 2D immiscible flow simulator and up-scaling methods were programmed with C++ programming language.

Material balance checks (less than 10-6 at each time step) assure that negligible convergence error of pressure and saturation equations are maintained during the simulations. In addition, cross check of fine scale numerical results of breakthrough time and water cut in a simple 1-D horizontal water flooding case with analytical Buckley-Leverett solution is performed to confirm the reliability and validity of our developed simulator. This is the widely used analytical benchmark for any new numerical simulator assessment. The simulator is then used to run different water flooding scenarios under different upscaling methods at various levels the performance of which are evaluated against fine scale results as the grand truth base.

Up-scaling Methods Evaluation

In order to evaluate up-scaling methods, it is required to compare results of fine grid simulation with corresponding coarse grid models. Moreover, several water flooding scenarios are performed on three heterogeneous reservoirs. Furthermore, the models are only heterogeneous in their absolute permeability distributions. Fig. 2 shows permeability distribution of reservoirs having×blocks.

They are generated using fractal fBm function. Moreover, not only can this method produce heterogeneous patterns, but also it can represent long range correlations among data (Mehrabi et al. [57]).

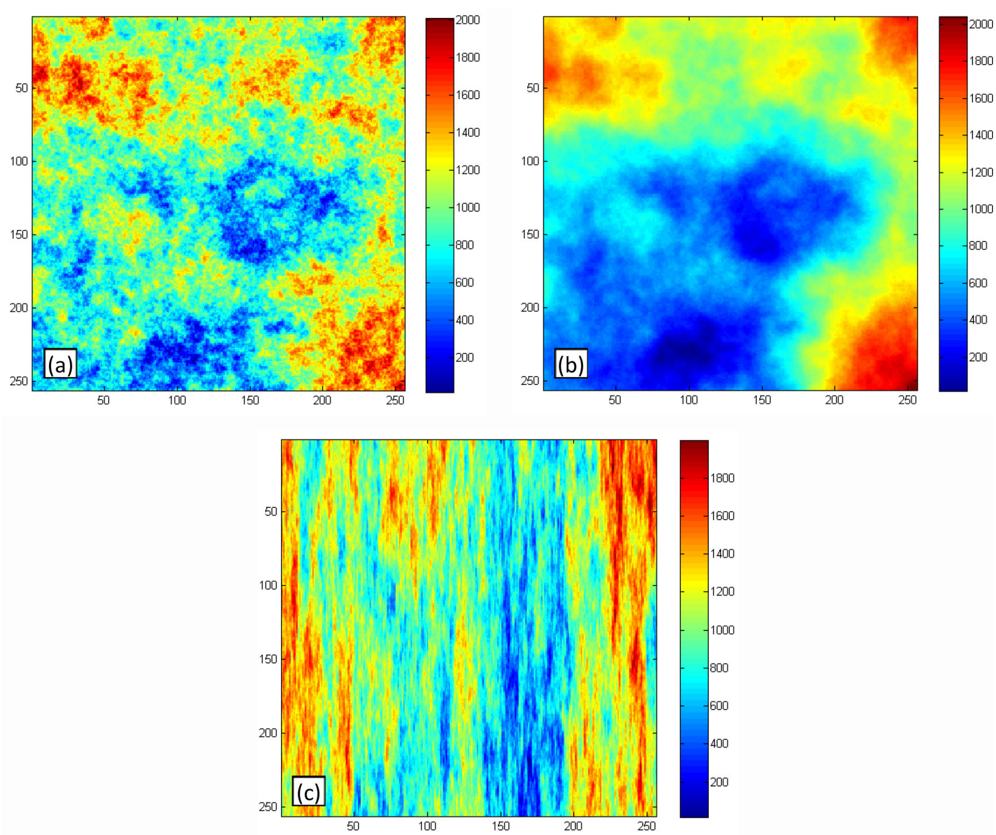

Fig. 2 Permeability distribution (md) of synthetic reservoirs 1 (a), 2 (b), and 3 (c).

Three permeability distributions with negative correlation (H=0.2), positive correlation (H=0.8), and anisotropic (layered) pattern (H=0.2) are used in different scenarios to investigate up-scaling performance under these different heterogeneities, where, Hurst exponent (H) is dimensionless. Statistical and fBm parameters of generated reservoirs are given in Table 1.

Simulation Scenarios

Durlofsky [54] states that for moderate degrees of coarsening, single-phase upscaling techniques often provide acceptable results, particularly when used in conjunction with specialized (flow-based) coarse grids. Therefore, six diagonal water flooding scenarios are designed in models with different mobility ratios, capillary pressure and heterogeneity characteristics. Moreover, these scenarios are utilized to evaluate up-scaling performance of different methods in different levels disregarding upscaling two-phase flow parameters such as relative permeability and capillary pressure. However, these scenarios are designed to force upscaling methods to face different processes. Furthermore, specifications of these models are given in Table 2. Ignoring capillary pressure, oil and water viscosities are changed to obtain mobility ratios of 20, 2, and 0.2 for the first three scenarios. In addition, capillary pressure is considered in the fourth scenario. These four scenarios are performed on reservoir 1 (H=0.2). Also, the other two scenarios are performed on reservoir 2 (H=0.8) and reservoir 3 (layered) to study the effects of heterogeneity pattern on up-scaling performance. Fluids and rock are considered incompressible. Parameters of Corey equation are given in Table 3.
Water injection rate is 3000 bbl/day for all scenarios. Production is continued until final water cut of 98%. In all scenarios, water is injected from the top left-side and production occurs from the bottom right-side of the models. Fig. 3 shows schematic of the reservoir with its production and injection openings.

Table 1 Statistical and fBm parameters of reservoirs permeability (md).

Reservoir	Average perm. (md)	Standard deviation of perm. (md)	Minimum perm. (md)	Maximum perm. (md)	Hurst exponent
1	975.52	315.89	0.1	2029.7	0.2
2	849.42	403.09	0.1	2056.4	0.8
3	1013.80	314.71	0.1	2014.8	0.2 (anisotropic)

Table 2 Characteristics of water flooding scenarios.

Scenario	Reservoir	Oil viscosity (cp)	Water viscosity (cp)	Production period (day)	Capillary pressure (psi)
1	1	3	1	6000	Zero
2	1	30	1	7000	Zero
3	1	0.3	1	3000	Zero
4	1	3	1	4000	Non zero
5	2	3	1	6000	Zero
6	3	3	1	6000	Zero

Table 3 Oil and water relative permeability parameters of Corey correlation.

Fluid	Residualsaturation	Reference relative permeability	Saturation exponent (n)
Oil	0.15	0.9	2
Water	0.20	0.6	2

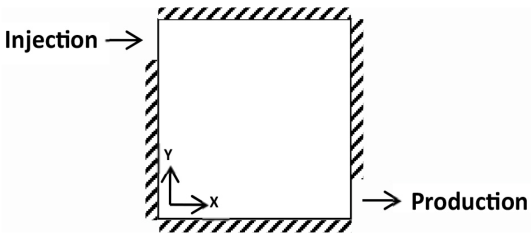

Fig. 3 Schematic of the reservoir with its production and injection openings.

Production boundary is considered at constant pressure of 3000 psi. Initial oil saturation and reservoir pressure are set to 0.8 and 3000 psi, respectively. Furthermore, coarsened models are generated by eight previously described methods in each scenario. Moreover, up-scaling is performed in four levels called 2, 4, 8, and 16. Furthermore, the name of each level points to the number of blocks which are up-scaled in each direction in a coarse block. Totally, 198 models are run. Up-scaling error of the models is calculated as follow (Equation 9):

$$E_r = \frac{C_c - C_f}{C_f} \times 100\% \qquad (9)$$

In which C_c and Cf are quantities of simulation results of coarse and fine reservoirs. Furthermore, it will be observed that error values are averaged over time to compare upscaling methods. One of the advantages of Equation 9 is that it produces both negative and positive error values over the time, and averaging these error values provides insight into whether the upscaling method generally underestimates or overestimates actual values.

Results and Discussion

Simulation results of the fine and coarse models in scenario 1 are presented in Fig. 4. Also, average reservoir pressure, injection boundary pressure and produced water and oil rates with dimensionless time are shown in Fig. 4.

Dimensionless time is the number of pore volume of water injected in the reservoir. Only arithmetic up-scaling method in levels 2, 4, 8, and 16 are shown. Also, abrupt pressure increase is due to fluid and rock incompressibility. In addition, good pressure match between fine and coarse models in levels 2 and 4 is obtained. Furthermore, pressure error is, however, considerably high for coarse models in next levels. Moreover, water and oil production rates of coarse models (in all up-scaling levels) follow closely those of the fine model (Fig. 4). This indicates good performance of arithmetic method and effectiveness of TVD approach. Pressure and water saturation distributions of fine and coarse models, averaged via arithmetic method, after 400 days of production are shown in Figs. 5 and 6. Good qualitative agreement between fine and coarse models is obtained.

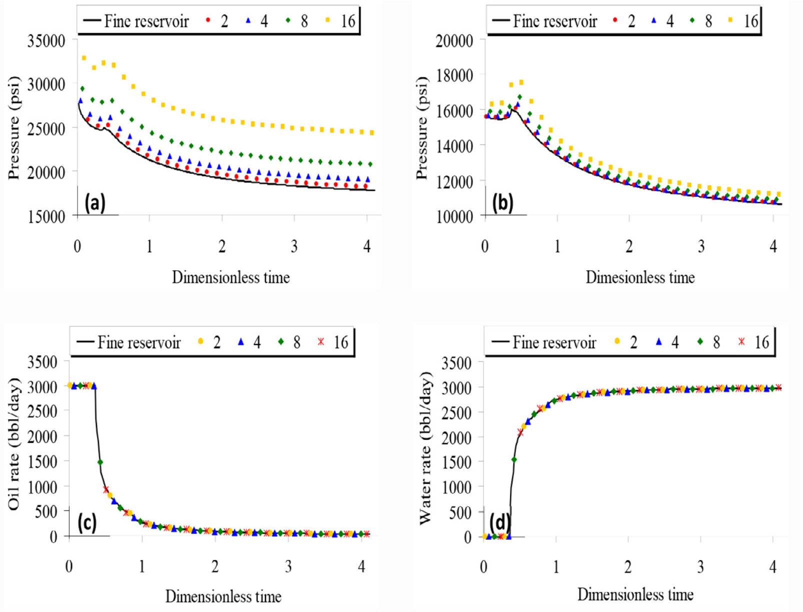

Fig. 4 Comparison between fine and different up-scaled models of reservoir 1 with arithmetic method for: (a) injection boundary pressure, (b) average reservoir pressure, (c) oil production rate and, (d) water production rate.

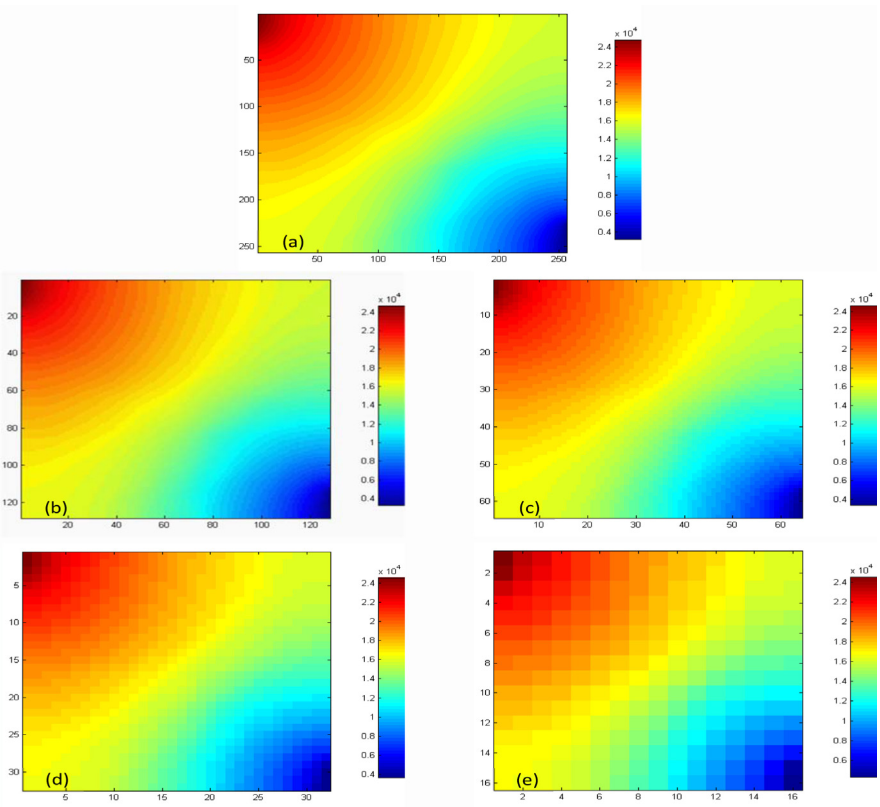

Fig. 5 Pressure distribution after 400 days for: (a) fine reservoir, and different up-scaled reservoirs by arithmetic method (b) level 2, (c) level 4, (d) level 8, and (e) level 16.

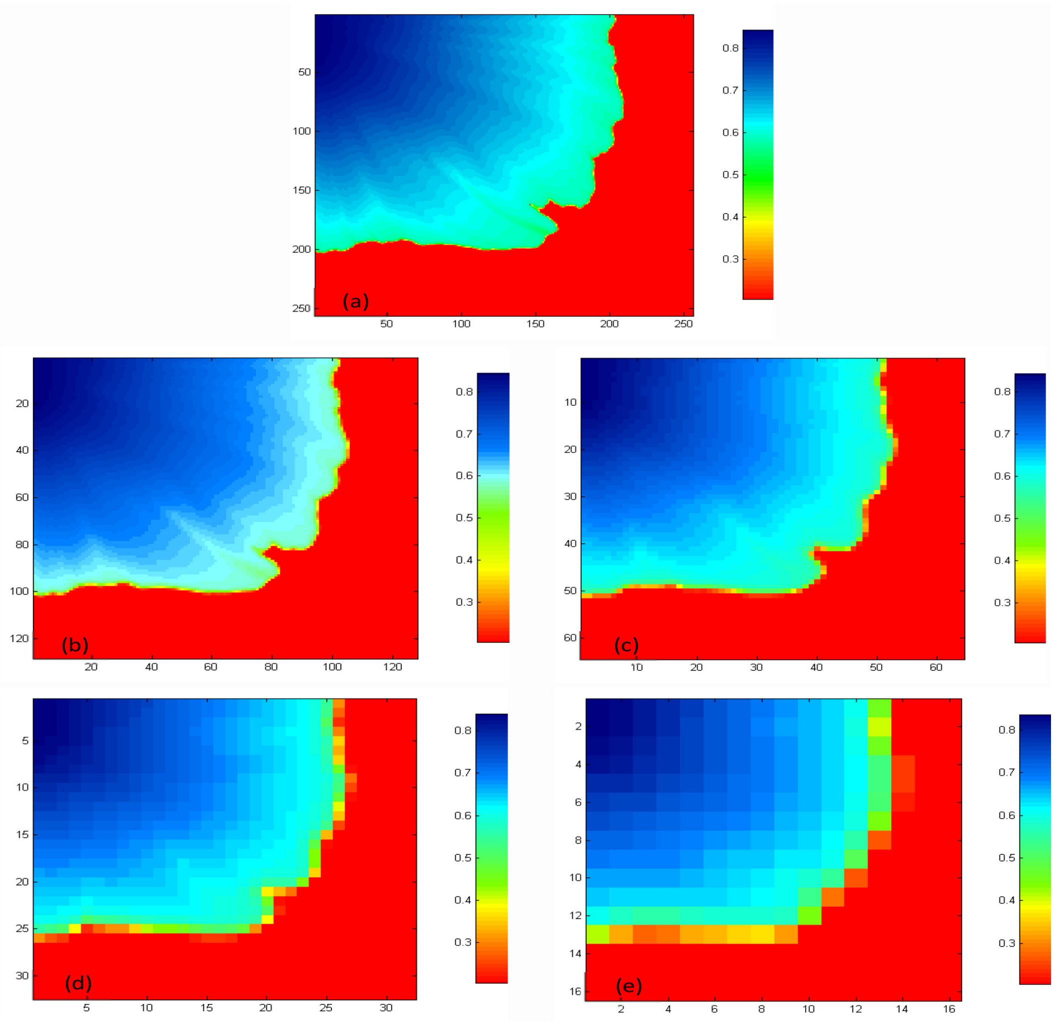

Fig. 6 Water saturation distribution after 400 days for: (a) fine reservoir, and different up-scaled reservoirs by arithmetic method (b) level 2, (c) level 4, (d) level 8, and (e) level 16.

Quantitative evaluation of up-scaling methods is possible using error curves of reservoir pressure, boundary pressure, water, and oil production rates. Moreover, error curves are obtained from Equation 3 in different times. Furthermore, maximum errors occur near breakthrough time. In addition, mismatch of breakthrough time in coarse and fine models produces large errors in all pressure and rate parameters. Also, errors are reduced sharply before and after breakthrough time. Overall performance of up-scaled models can be quantified by averaging error values during simulation time. Moreover, up-scaled models can be compared through these averaged errors in each level. Furthermore, average error bar charts are generated for these comparative studies as shown in Fig. 7 for the first scenario.

These charts are generated for boundary pressure, average pressure, oil and water production rates. For each property, error charts are developed for coarse models constructed with 8 up-scaling methods in 4 up-scaling levels. Inspection of Fig. 7 reveals that average boundary pressure errors are high and increase rapidly with up-scaling level from 2% at level 2 to 35% at level 16. Similar behavior is observed for average reservoir pressure, but with much smaller errors up to 7% at up-scaling level 16.

All the pressure errors are positive which it shows that up-scaled models always over-predict the pressure values. Although the precise values or amounts of pressure errors have not been presented by us in this study, similar high-pressure errors were obtained in all scenarios. This shows that no absolute permeability up-scaling method is good enough for proper pressure match between fine and high-level coarse models. Special near well/near boundary up-scaling methods are, therefore, necessary for this purpose. The concept of near boundary upscaling has not been developed yet, but many near-well up-scaling methods have been proposed so far [58, 59]. Since no well is presented in the models, these methods have not been implemented in this study.

Average errors in oil and water production rates are very small and never exceeded 0.27% in the worst case of scenario 1. No systematic over- or under-prediction is observed in these parameters and errors are generally increased with up-scaling level.

Again, by averaging errors of four up-scaling levels, overall averaged error of each method can be generated for the models. The averaged errors corresponding to four upscaling levels, under different scenarios accounting for the effects of heterogeneity, capillary forces, and mobility ratio, are reported in Tables 4 and 5 for water and oil production rates, respectively.

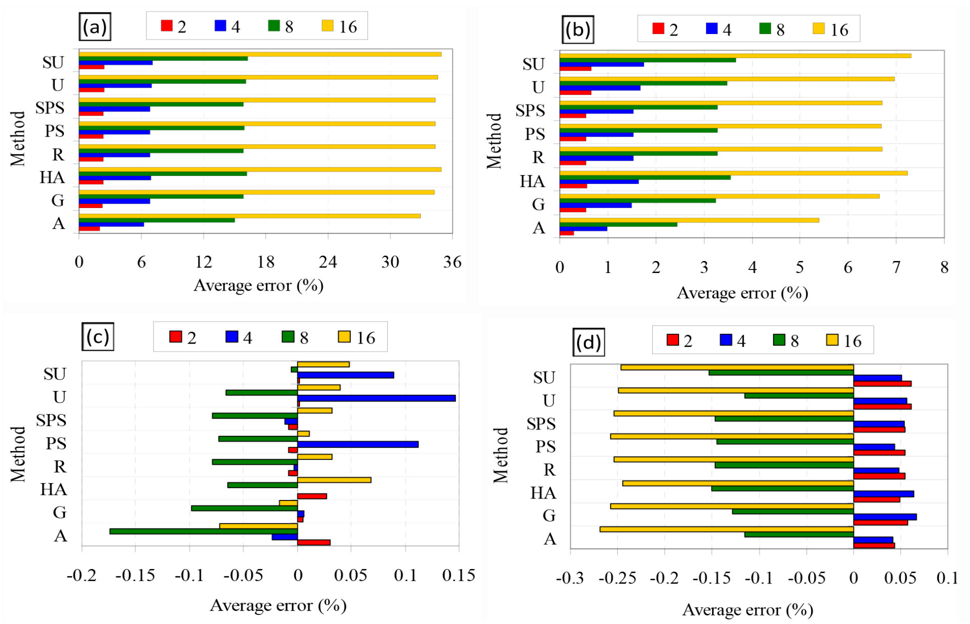

Fig. 7 Average error of up-scaling methods in scenario 1 and up-scaling levels 2, 4, 8, and 16 for: (a) injection boundary pressure, (b) reservoir average pressure, (c) oil production rate and (d) water production rate.

Table 4 Averaged errors of four levels of upscaling methods for water production rate under different scenarios, accounting for the effects of heterogeneity, capillary forces, and mobility ratio.

	Heterogeneity			Capillary pressure		Mobility ratio		
Upscaling	Res. 1	Res. 2	Res. 3	Pc=0	Pc≠0	MR=0.2	MR=2	MR=20
method	Scenario 1	Scenario 5	Scenario 6	Scenario 1	Scenario 4	Scenario 3	Scenario 1	Scenario 2
A	-0.075	0.029	0.156	-0.075	-0.086	1.281	-0.075	0.204
G	-0.065	0.059	0.165	-0.065	-0.086	1.448	-0.065	0.191
HA	-0.071	0.060	0.180	-0.071	-0.083	1.545	-0.071	0.198
R	-0.075	0.058	0.173	-0.075	-0.082	1.476	-0.075	0.185
PS	-0.076	0.054	0.176	-0.076	-0.082	1.461	-0.076	0.207
SPS	-0.073	0.057	0.172	-0.073	-0.084	1.476	-0.073	0.185
U	-0.061	0.060	0.184	-0.061	-0.074	1.527	-0.061	0.193
SU	-0.072	0.071	0.187	-0.072	-0.086	1.556	-0.072	0.196

Table 5 Averaged errors of four levels of upscaling methods for oil production rate under different scenarios, accounting for the effects of heterogeneity, capillary forces, and mobility ratio.

	Heterogeneity			Capillary pressure		Mobility ratio		
Upscaling	Res. 1	Res. 2	Res. 3	Pc=0	Pc≠0	MR=0.2	MR=2	MR=20
method	Scenario 1	Scenario 5	Scenario 6	Scenario 1	Scenario 4	Scenario 3	Scenario 1	Scenario 2
A	-0.060	-0.442	-0.093	-0.060	-0.083	5.651	-0.060	0.288
G	-0.026	-0.269	-0.116	-0.026	-0.027	5.861	-0.026	0.255
HA	0.008	-0.293	-0.038	0.008	0.000	6.050	0.008	0.255
R	-0.015	-0.339	-0.018	-0.015	-0.038	5.859	-0.015	0.263
PS	0.010	-0.323	-0.021	0.010	-0.015	5.885	0.010	0.269
SPS	-0.017	-0.334	0.018	-0.017	-0.008	5.859	-0.017	0.266
U	0.030	-0.224	-0.002	0.030	-0.025	5.962	0.030	0.266
SU	0.033	-0.162	-0.031	0.033	0.012	6.036	0.033	0.253

The bar charts of these error values for oil and water production rates, categorized according to the contribution of heterogeneity, capillary forces, and mobility ratio, are depicted in figures 8 to 10.

As shown in Fig. 8-a, oil production errors are more pronounced in reservoir 2, where several upscaling methods exhibit negative deviations from the reference solution, while reservoirs 1 and 3 remain closer to zero error. In contrast, for water production (Fig. 8-b), the errors are generally smaller, with reservoir 3 tending to show slightly higher positive deviations, and reservoir 1 showing slightly negative errors. Overall, the dispersion of errors in water production is lower compared to oil production, indicating that upscaling is more robust for water prediction under heterogeneity effects.

The inclusion of capillary pressure increases the error levels in both oil and water production (Fig. 9). As illustrated in Fig. 9-a, its influence on oil production is relatively limited, with most upscaling methods showing errors close to zero. In contrast, for water production (Fig. 9-b), the impact of capillary pressure is more pronounced: all methods display negative errors, and the inclusion of Pc slightly increases the deviation from the reference solution. This indicates that water production predictions are more sensitive to capillary effects than oil production.

As illustrated in Fig. 10, the upscaling errors are strongly dependent on the mobility ratio. For MR = 0.2, all methods yield significant errors, reaching up to 5–6% for oil and around 1.5% for water production rates. In contrast, for MR = 2 and MR = 20, the errors are negligible in both oil and water production, indicating that the impact of mobility ratio is much more pronounced when MR < 1.

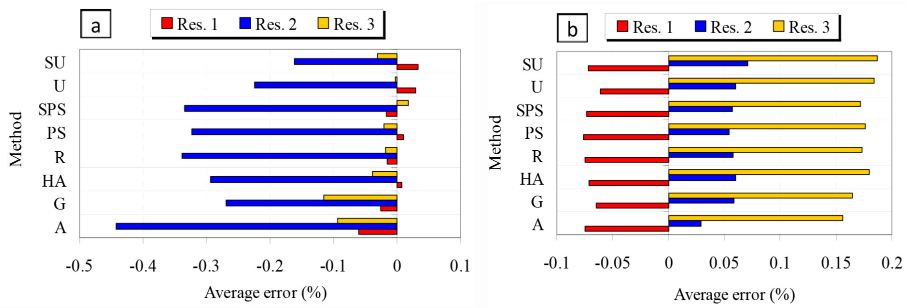

Fig. 8 Bar chart of averaged errors for four upscaling levels in (a) oil production rate and (b) water production rate, accounting for the contribution of heterogeneity, for scenarios 1, 5, and 6 (reservoirs 1-3).

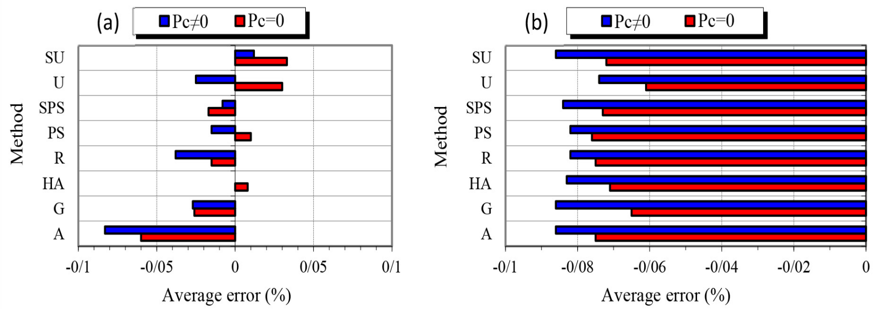

Fig. 9 Bar chart of averaged errors for four upscaling levels in (a) oil production rate and (b) water production rate, accounting for the contribution of capillary forces, for scenarios 1 and 4.

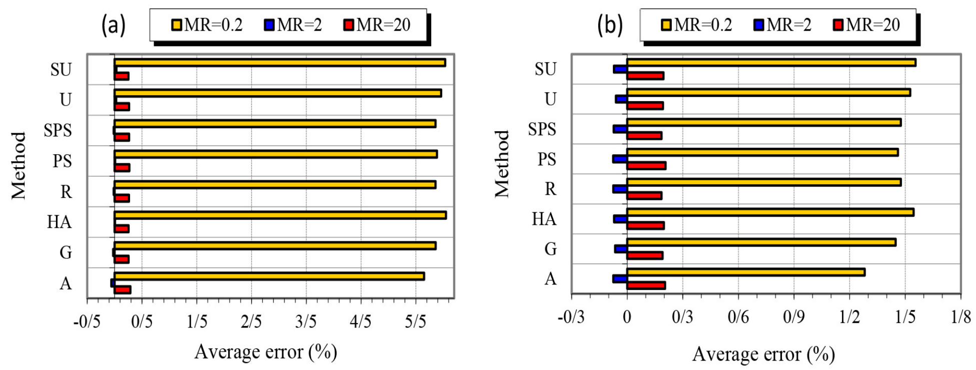

Fig. 10 Bar chart of averaged errors for four upscaling levels in (a) oil production rate and (b) water production rate, accounting for the contribution of mobility ratio, for scenarios 1-3.

These charts can also be used to perform comparative analysis between upscaling methods under different scenarios. The performance of these methods, with respect to the effect of heterogeneity, capillary pressure, and mobility ratio, is presented in Tables 6 to 8, respectively.

In these tables, the methods are ranked based on the overall average error values, as reported in Tables 4 to 5 and illustrated in Fig.s 8 to 10. Also, approximation sign (≈) in these tables shows equal performance of the methods. Moreover, inspection of these tables shows good performance of all the upscaling methods. Furthermore, numerical methods gave smaller overall error than analytical methods in most scenarios. In addition, unbiased and sequential unbiased are the superior numerical methods and arithmetic and harmonic-arithmetic methods are the superior analytical methods.

An important issue in any upscaling method, other than its accuracy, is the computation speed up factor of the method relative to the fine model simulation. Moreover, (1) simulation run time and (2) speed up factors of arithmetic method is presented in Tables 9 and 10 for different scenarios and up-scaling levels, respectively.

Table 6 Ranking of up-scaling methods in different heterogeneities based on minimum error for oil and water production rate.

Produced fluid	Heterogeneity	Ranking of methods
Oil	Res. 1	HA < PS < R < SPS < G < U < SU < A
	Res. 2	SU < U < G < HA < PS < SPS < R < A
	Res. 3	U < R ≈ SPS < PS < SU < HA < A < G
Water	Res. 1	U < G < SPS ≈ HA ≈ SU < R ≈ PS ≈ A
	Res. 2	A < PS < SPS ≈ G ≈ R < HA ≈ U < SU
	Res. 3	A < G < R ≈ SPS < PS < HA < U < SU

Table 7 Ranking of up-scaling methods with and without capillary pressure in reservoir1 based on minimum error for oil and water production rate.

Produced fluid	Capillary pressure	Ranking of methods
Oil	Zero	HA < PS < R < SPS < G < U < SU < A
	Non-zero	HA < SPS < SU < PS < U < G < R < A
Water	Zero	U < G < SPS ≈ HA ≈ SU < R ≈ PS ≈ A
	Non zero	U < PS ≈ R < SPS ≈ HA < G ≈ SU ≈ A

Table 8 Ranking of up-scaling methods in different mobility ratios in reservoir 1 based on minimum error for oil and water production rate.

Produced fluid	Mobility ratio	Ranking of methods
Oil	0.2	A < G ≈ R ≈ SPS < PS < U < SU < HA
	2	HA < PS < R < SPS < G < U < SU < A
	20	SU < U ≈ SPS ≈ PS ≈ R ≈ HA ≈ G < A
Water	0.2	A < G < PS < R ≈ SPS < U < HA ≈ SU
	2	U < G < SPS ≈ HA ≈ SU < R ≈ PS ≈ A
	20	R ≈ SPS < G < U < SU ≈ HA < A ≈ PS

Table 9 Simulation run time in different scenarios for fine and coarse reservoirs, up-scaled by arithmetic method.

Scenario	Simulation Run Time (Second)				
	Fine Reservoir	Upscaling Level of Coarse reservoir			
		2	4	8	16
1	114665	4838	504	78	36
2	1698084	102580	10775	1532	292
3	156726	6938	628	86	17
4	106446	4579	468	73	34
5	123981	5507	479	82	35
6	93835	4340	479	77	35

Table 10 Speed-up factors in different scenarios and up-scaling levels of arithmetic method.

Scenario	Upscaling Level			
	2	4	8	16
1	23	227	1470	3185
2	16	157	1108	5815
3	22	249	1822	9219
4	23	227	1458	3130
5	22	258	1511	3542
6	21	195	1218	2681

Obtained speed-ups depend on up-scaling level and reach to 3 orders of magnitude after 3 levels. This approach is, certainly, attractive and can be considered as a cost-effective alternative for parallelization when dynamic simulations of multimillion-block geological models are required.

Conclusions

Eight absolute permeability up-scaling methods were evaluated. Three numerical up-scaling methods namely unbiased, sequential-unbiased, and sequential pressure solver, were presented for the first time. Six water flooding scenarios have been performed over three synthetic reservoirs. Moreover, permeability distributions were generated using Fractal fBm function with negative correlation (H=0.2), positive correlation (H=0.8), and anisotropic (layered) pattern (H=0.2). Also, processes with broad range of mobility ratios from 0.2 to 20 with and without capillary pressure were investigated. It was observed that pressure match was not very satisfactory for coarsened models especially at high up-scaling levels. Furthermore, average boundary pressure errors were high and increased rapidly with up-scaling level from 2% at level 2 to 35% at level 16. Similar behavior was observed for average reservoir pressure, but with much smaller errors up to 7% at up-scaling level 16. Therefore, it is necessary to apply specific near-well/ near-boundary up-scaling methods to improve pressure distribution in coarse models. Moreover, except near their breakthrough time, fine and course models showed good to fair agreement for production rates of both oil and water. In addition, the overall error of the coarse models never exceeded 0.5% with respect to heterogeneity and capillary pressure effects, whereas at MR = 0.2, it increased to about 5–6% for oil and 1.5% for water production rate. Upscaling methods were ranked based on the overall average error under scenarios involving heterogeneity, capillary forces, and mobility ratio. Also, numerical methods gave smaller overall error compared to analytical methods in most scenarios. Moreover, unbiased and sequential unbiased were found to be the superior numerical methods and arithmetic and harmonic-arithmetic methods were identified as the superior analytical methods. Furthermore, speed-up factors depend on up-scaling level and was around 20 after 1 level and reached up to 3 orders of magnitude after 3 levels.

Nomenclatures

A (ft^2): Area
P_c (psi): Capillary pressure
C_c: Coarse reservoir simulation results
C_f: Fine reservoir simulation results
Q: (bbl/day): Flow rate
H: (dimensionless): Hurst exponent
nw: Index of non-wet phase
w: Index of wet phase,
Q_{in}:(bbl/day): Inlet flow rate
Pi_n: (psi): Inlet pressure,
L (*ft*): Length
D: Number of dimensions
m: Number of upscaling level
P_{out}(psi): Outlet pressure
K (*md*): Permeability
λ: Positive number,
k_{r0}: Maximum (reference) relative permeability,
E_r (%): Relative error
k_r: Relative permeability
S_r: Residual saturation
n: Saturation exponent
S: Saturation
P_{th} (psi): Threshold pressure
μ (cP): Viscosity
HA: Harmonic-Arithmetic
IMPES: Implicit pressure and explicit saturation
SPS: Sequential Pressure-Solver
SU: Sequential Unbiased

References

1. Matheron, G. (1967). Éléments pour une théorie des milieux poreux, 1st edition, Masson et Cie, Paris, 1-168.
2. Muskat, M. (1937). The flow of homogeneous fluids through porous media. 1st edition. McGraw-Hill Book Co., New York, 1-763.
3. Bouwer, H. (1969). Planning and interpreting soil permeability measurements, Journal of the Irrigation and Drainage Division of the A.S.C.E., 95(3), 391–402, doi.org/10.1061/JRCEA4.0000661.
4. Warren, J. E., & Price, H. S. (1961). Flow in heterogeneous porous media, Journal of Petroleum Technology, 1(3), 153–169, doi.org/10.2118/1579-g.
5. Dagan, G. (1982). Stochastic modeling of groundwater flow by unconditional and conditional probabilities: 1. Conditional simulation and the direct problem. Water Resources Research, 18(4), 813–833, doi.org/10.1029/WR018i004p00813.
6. Dagan, G. (1985). Stochastic modeling of groundwater flow by unconditional and conditional probabilities: 2.

The inverse problem. Water Resources Research, 21(1), 65–72, doi.org/10.1029-/WR021i001p00065.

7. Dagan, G. (1989). Flow and Transport in Porous Formations. 1st edition, Springer-Verlag, New York, 1-465.
8. Clifton, P. M., & Neuman, S. P. (1982). Effects of kriging and inverse modeling on conditional simulation of the Avra Valley Aquifer in southern Arizona, Water Resources Research, 18(4), 1215–1234, doi:10.1029/WR018i004p01215.
9. Journel, A. G., Deutsch, C., & Desbarats, A. J. (1986). Power averaging for block effective permeability, SPE California Regional Meeting, Oakland, California.
10. 10. Durlofsky, L. J. (1992). Representation of grid block permeability in coarse scale models of randomly heterogeneous porous media. Water Resources Research, 28(7), 1791–1800, doi.org/10.1029/-92WR00709.
11. Lozano, J. A., Costa, L. P., Alves, F. B., & Silva, A. C. (1996). Upscaling of stochastic models for reservoir simulation-An integrated approach, Abu Dhabi International Petroleum Exhibition and Conference, Abu Dhabi, United Arab Emirates.
12. Pickup, G. E., & Sorbie, K. S. (1996). Scaleup of two-phase flow in porous media using phase permeability tensors. SPE Journal, 1(4), 369–382, doi.org/10.2118/28586-PA.
13. Sharifi, M., & Kelkar, M. (2013). New dynamic permeability upscaling method for flow simulation under depletion drive and no-crossflow conditions. Petroleum Science, 10(2), 233–241, doi.org/10.1007/s12182-013-0272-7.
14. Hsieh, A. I., Allen, D. M., & MacEachern, J. A. (2017). Upscaling permeability for reservoir-scale modeling in bioturbated, heterogeneous tight siliciclastic reservoirs: Lower Cretaceous Viking Formation, Provost Field, Alberta, Canada. Marine and Petroleum Geology, 88, 1032–1046. doi.org/10.1016/j.marpetgeo.2017.09.023
15. King, P. R. (1989). The use of renormalization for calculating effective permeability. Transport in Porous Media, 4(1), 37–58, doi.org/10.1007/BF00134741.
16. 16. Green, C. P., & Paterson, L. (2007). Analytical three-dimensional renormalization for calculating effective permeabilities. Transport in Porous Media, 68(2), 237–248. doi.org/10.1007/s11242-006-9042-y
17. Karim, M. R., & Krabbenhoft, K. (2010). New renormalization schemes for conductivity upscaling in heterogeneous media. Transport in Porous Media, 85(3), 677–690. doi.org/10.1007/s11242-010-9585-9
18. Liao, Q., Lei, G., Wei, Z., Zhang, D., & Patil, S. (2020). Efficient analytical upscaling method for elliptic equations in three-dimensional heterogeneous anisotropic media. Journal of Hydrology, 583, 124560, doi.org/10.1016/j.jhydrol.2020.124560.
19. Liao, Q., Li, G., Tian, S., Song, X., Lei, G., Liu, X., Chen, W., & Patil, S. (2023). An efficient analytical approach for steady-state upscaling of relative permeability and capillary pressure. Journal of Energy, 282, 128426, doi.org/10.1016/j.energy.2023.128426.
20. Gomez-Hernandez J. J. (1991). A Stochastic Approach to The Simulation of Block Conductivity Fields Conditioned upon Data Measured at a Smaller Scale, PhD thesis, Stanford University, California, United States of America, 1-351.
21. Sánchez-Vila, X., Girardi, J. P., & Carrera, J. (1995). A synthesis of approaches to upscaling of hydraulic conductivities. Water Resources Research, 31(4), 867–882, doi.org/10.1029-/95WR00882.
22. White, C. D., & Horne, R. N. (1987). Computing absolute transmissibility in the presence of fine-scale heterogeneity. SPE Symposium on Reservoir Simulation, San Antonio, Texas, USA.
23. Lunati, I., Bernard, D., Giudici, M., Parravicini, G., & Ponzini, G. (2001). A numerical comparison between two upscaling techniques: non-local inverse based scaling and simplified renormalization. Advances in Water Resources, 24(8), 913–929, doi.org/10.1016/S0309-1708(01)00008-2.
24. McCarthy, J. F. (1991). Analytical models of the effective permeability of sand-shale reservoirs. Geophysical Journal International, 105(2), 513–527, doi.org/10.1111/j.1365-246X.1991.tb06730.x. 20
25. Wen, X. H., & Gómez-Hernández, J. J. (1996). Upscaling hydraulic conductivities in heterogeneous media: An overview. Journal of Hydrology, 183(1–2), ix–xxxii, doi.org/10.1016/S0022-1694(96)80030-8.
26. Renard, P., & de Marsily, G. (1997). Calculating equivalent permeability: A review. Advances in Water Resources, 20(5–6), 253–278, doi.org/10.1016/S0309-1708(96)00050-4.
27. Durlofsky, L. J. (2005). Upscaling and gridding of fine scale geological models for flow simulation, 8th International Forum on Reservoir Simulation, Iles Borromees, Stresa, Italy.
28. Chen, Y., Durlofsky, L. J., Gerritsen, M., & Wen, X. H. (2003). A coupled local-global upscaling approach for simulating flow in highly heterogeneous formations. Advances in Water Resources, 26, 1041–1060, doi.org/10.1016/S0309-1708(03)00101-5.
29. Chen, Y., & Durlofsky, L. J. (2006). Adaptive local–global upscaling for general flow scenarios in heterogeneous formations. Transport in Porous Media, 62(2), 157–185, doi.org/10.1007/s11242-005-0619-7.
30. Zhou, H., Li, L., & Gómez-Hernández, J. J. (2010). Three-dimensional hydraulic conductivity upscaling in groundwater modeling. Computers & Geosciences, 36(10), 1224–1235, doi.org/10.1016/-j.cageo.2010.04.001.
31. Chen T. (2009). New methods for accurate upscaling with full-tensor effects, Ph.D. dissertation, Stanford University, California, United States of America, 1-118.
32. Dagan, G., Fiori, A., & Jankovic, I. (2013). Upscaling of flow in heterogeneous porous formations: Critical examination and issues of principle. Advances in Water Resources, 51, 67–85, doi.org/10.1016/j.advwatres.2012.12.017.
33. Suribhatla, R., Jankovic, I., Fiori, A., Zarlenga, A., & Dagan, G. (2011). Effective conductivity of an anisotropic heterogeneous medium of random conductivity distribution. Multiscale Modeling & Simulation, 9(3), 933–954, doi.org/10.1137/100805662.
34. Jankovic, I., Fiori, A., & Dagan, G. (2013). Effective

conductivity of isotropic highly heterogeneous formations: Numerical and theoretical issues. Water Resources Research, 49(2), 1178–1183, doi.org/10.1029/2012WR012441.

35. Fouda, M. A. G. (2016). Relative permeability upscaling for heterogeneous reservoir models, Ph.D. dissertation, Heriot-Watt University, Edinburgh, UK, 1–178.
36. Evazi, M., & Jessen, K. (2014). Dual-porosity coarse-scale modeling and simulation of highly heterogeneous geomodels. Transport in Porous Media, 105, 211–233, doi.org/10.1007/s11242-014-0367-7.
37. Failla, A. (2015). A numerical upscaling technique for absolute permeability and single phase flow based on the finite difference method, MSc thesis, Politecnico di Milano, Milan, Italy.
38. Mazo, A. B., & Potashev, K. A. (2018). Absolute permeability upscaling for superelement modeling of petroleum reservoir. Mathematical Models and Computer Simulations, 10(1), 26–35. doi.org/10.1134/S20700482-1801009X
39. Li, H., & Durlofsky, L. J. (2016). Ensemble level upscaling for compositional flow simulation. Computational Geosciences, 20(3), 525–540, doi.org/10.1007/s10596-015-9503-x.
40. Vitel, S., & Souche, L. (2007). Unstructured upgridding and transmissibility upscaling for preferential flow paths in 3D fractured reservoirs. Paper SPE-106483-MS, presented at the SPE Reservoir Simulation Symposium, 26–28 February 2007, Houston, Texas, USA.
41. Lambers, J. V., Gerritsen, M. G., & Mallison, B. T. (2008). Accurate local upscaling with variable compact multipoint transmissibility calculations. Computational Geosciences, 12(3), 399–416. doi.org/10.1007/s10596-007-9068-4
42. Azmi, H., Willuweit, M., Ramli, A., & Barkve, T. (2016). Scale handling from geo model to flow model with focus on transmissibility upscaling and fault seal upscaling challenges. In Proceedings of the Third EAGE Integrated Reservoir Modelling Conference (pp. 1–4). European Association of Geoscientists & Engineers. doi.org/10.3997/2214-4609.201602439
43. Guérillot, D., & Bruyelle, J. (2014). A fast and accurate upscaling of transmissivities for field scale reservoir simulation. In Proceedings of ECMOR XIV – 14th European Conference on the Mathematics of Oil Recovery (pp. 1–16). Catania, Sicily, Italy, 8–11 September 2014. European Association of Geoscientists & Engineers. doi.org/10.3997/2214-4609.20141863
44. Guérillot, D., & Bruyelle, J. (2019). Transmissibility Upscaling on Unstructured Grids for Highly Heterogeneous Reservoirs. Water, 11(12), 2647. doi.org/10.3390/w11122647
45. Alpak, F. O. (2021). Practical implementation of a method for global single-phase flow-based transmissibility upscaling using generic flow boundary conditions and its application on models with non-local heterogeneities. Journal of Petroleum Science and Engineering, 207, 109037. doi.org/10.1016/j.petrol.2021.109037
46. Stone, M. T., Wu, X. H., Parashkevov, R. R., & Lyons, S. L. (2007). Challenges and solutions in global-flow-based scaleup of permeability: isolated flow bodies, SPE Reservoir Simulation Symposium, Houston, Texas, USA.
47. Kumar D. (2014). Modeling Steam Assisted Gravity Drainage in Heterogeneous Reservoirs Using Different Upscaling Techniques, MSc thesis, The University of Texas at Austin, Texas, United States of America, 1–100.
48. Kumar, D., Murugesu, M., & Srinivasan, S. (2014). Modeling effect of permeability heterogeneities on SAGD performance using improved upscaling schemes. In SPE Heavy Oil Conference–Canada 2014 (pp. 1318–1335). Society of Petroleum Engineers. doi.org/10.2118/170115-MS
49. Murugesu, M. (2015). Improved upscaling scheme for steam assisted gravity drainage (SAGD) and semi-analytical modeling of the SAGD rising phase. MSc thesis, The University of Texas at Austin, Austin, Texas, USA.
50. Tan, Q., Liu, S., Hu, Z., Li, H., & Sun, B. (2025). A novel upscaling method for steam-assisted gravity drainage simulations based on viscosity-temperature model. Petroleum Geoscience. Advance online publication. doi.org/10.1144/petgeo2025-033
51. Dehghan Khalili, A., Arns, J.-Y., Hussain, F., Cinar, Y., Pinczewski, W., & Arns, C. H. (2013). Permeability upscaling for carbonates from the pore scale by use of multiscale X-Ray-CT images. SPE Reservoir Evaluation & Engineering, 16(04), 353–368. doi.org/10.2118/152640-PA
52. Bashtani, F., Taheri, S., & Kantzas, A. (2018). Scale up of pore-scale transport properties from micro to macro scale; network modelling approach. Journal of Petroleum Science and Engineering, 170, 541–562, doi.org/10.1016/j.petrol.2018.07.001
53. Elmorsy, M., El-Dakhakhni, W., & Zhao, B. (2023). Rapid permeability upscaling of digital porous media via physics-informed neural networks. Water Resources Research, 59(12), e2023WR035064, doi.org/10.1029/-2023WR035064.
54. Durlofsky, L. J. (2003). Upscaling of Geocellular Models for Reservoir Flow Simulation: A Review of Recent Progress, 7th International Forum on Reservoir Simulation, Bühl/Baden-Baden, Germany.
55. Wallstorm, T. C., Hou, S., Christie, M. A., Durlofsky, L. J., and Sharp, D. H. (1998). Accurate Scale up of Two Phase Flow Using Renormalization and Nonuniform Coarsening, Technical Report LA-UR-98-2507, Los Alamos National Laboratory, Los Alamos, New Mexico, USA.
56. Oldenburg, C. M., & Pruess, K. (1999). Simulation of propagating fronts in geothermal reservoirs with the implicit Leonard total variation diminishing scheme. Geothermics, 29(1), 1–25.
57. Mehrabi, A. R., Rassamdana, H., & Sahimi, M. (1997). Characterization of long-range correlations in complex distributions and profiles. Physical Review E, 56(1), 712–722, doi.org/10.1103/-PhysRevE.56.712.
58. Ding, Y. (1995). Scaling-up in the vicinity of wells in heterogeneous field, 13th SPE Symposium on Reservoir Simulation, San Antonio, Texas, USA, 441-451.
59. 59. Durlofsky, L. J., Milliken, W. J., & Bernath, A. (2000). Scaleup in the near-well region. SPE Journal, 5(1), 110–117, doi.org/10.2118/61855-PA.